

## Assessing Canopy Phenological Variations and Gross Primary Productivity in A Savanna Ecosystem in Yuanjiang, Yunnan Province of Southwest China

S. T. Z. Myo<sup>1,3,4</sup>, Y. P. Zhang<sup>1,2,\*</sup>, Q. H. Song<sup>1,2,\*</sup>, A. G. Chen<sup>1,7</sup>, D. X. Yang<sup>1,7</sup>, L. G. Zhou<sup>1</sup>, Y. X. Lin<sup>1</sup>, Z. Phyo<sup>1,3,4</sup>, X. H. Fei<sup>5</sup>, and N. S. Liang<sup>6</sup>

<sup>1</sup> CAS Key Laboratory of Tropical Forest Ecology, Xishuangbanna Tropical Botanical Garden, Chinese Academy of Sciences, Xishuangbanna 666303, China

<sup>2</sup> Center of Plant Ecology, Core Botanical Gardens, Chinese Academy of Sciences, Xishuangbanna 666303, China

<sup>3</sup> University of Chinese Academy of Sciences, Beijing 100049, China

<sup>4</sup> Myanmar Timber Enterprise, Ministry of Natural Resources and Environmental Conservation, Yangon 11012, Myanmar

<sup>5</sup> College of Resources and Environmental Engineering, Guizhou University, Guiyang 550025, China

<sup>6</sup> Center for Global Environmental Research, National Institute for Environmental Studies, Tsukuba, Ibaraki 305-8506, Japan

<sup>7</sup> Yuanjiang Savanna Ecosystem Research Station, Xishuangbanna Tropical Botanical Garden, Chinese Academy of Sciences, Yuanjiang 653300, China

Received 23 January 2021; revised 29 November 2021; accepted 18 February 2022; published online 15 September 2023

**ABSTRACT.** Vegetation phenology is an important indicator of environmental change and strongly connected to forest ecosystem productivity change. This study aimed to analyse the pattern of phenological variations derived from digital imagery for the interpretation of ecosystem productivity. For 2014, 2015 and 2016, the seasonal phenological development of savanna was analysed by using tower-based imagery from a digital camera. The green excess index (GEI) was the best at representing the phenological transition dates (PTDs) and useful for investigating the gross primary production (GPP) in the savanna ecosystem. There was a significant correlation between the monthly pattern of the strength of green ( $S_{green}$ ), green excess index (GEI) and vegetation contrast index (VCI) and GPP throughout the year. Additionally, the annual pattern of colour indices had significant relationship ( $p < 0.05$ ) with GPP but this was not seasonal. The air temperature (air T) and soil temperature (soil T) were strongly significantly correlated ( $p < 0.001$ ) with the start of growing season (SGS) and caused the advance in green-up and the timing of the start of the growing season in 2014 and 2016. The short growing season length (GSL) had an impact on the productivity. The colour indices from the digital camera images not only provided the phenological pattern of a forest canopy but also revealed the forest ecosystem productivity by showing the response to environmental factors. Our results indicate that daily continuous digital camera images might be useful for ecologists to use as a tool for future prediction of the long-term phenological modelling.

**Keywords:** canopy phenology, digital image, colour indices, gross primary productivity, environmental factors, savanna

### 1. Introduction

The effects of environmental change on the terrestrial ecosystem are important for analysing the relationships between canopy phenological events and gross primary production (GPP) (Ito, 2010; Muraoka et al., 2010; Richardson et al., 2010; Polgar and Primack, 2011; Fridley, 2012). Phenological events are changed by environmental cues, such as temperature (Richardson et al., 2006; Vitasse et al., 2011; Gerst et al., 2017; Park et al., 2017), irradiance (Saleska et al., 2007), precipitation (Craine et al., 2012; Shen et al., 2015), and photoperiod (Basler and

Körner, 2012). Ground-based phenological observations are a traditional method for specific sites and species that can investigate phenological variations across a broad geographical range (Piao et al., 2019). However, these observation involve different observers and methods and are difficult to perform in some ecosystems since the results of phenological events are not uniform (Piao et al., 2019). Although satellite remote sensing techniques have also been widely applied in plant phenology to detect the timing of phenological events of greenness-related vegetation indices (Piao et al., 2019), multiple factors, such as poor observation conditions, clouds, snow and ice, bidirectional reflectance distribution function effects, shifts in sensors, and coarse spatial and temporal resolutions, can contribute to reducing the accuracy of satellite-derived estimates of plant phenological events (Piao et al., 2019). Recently, automatically captured digital camera images, a form of near-surface remote sensing, have been used as a tool to monitor vegetation phenology on the ecosystem scale. The digital camera collects automated data at high temporal resolution in multiple ecosystems with lower operating

\* Corresponding author. Tel.: +86 871-65160904; fax: +86 871-65160916. E-mail address: yipingzh@xtbg.ac.cn (Y. P. Zhang).

\* Corresponding author. Tel.: +86 871-65160904; fax: +86 871-65160916. E-mail address: sqh@xtbg.ac.cn (Q. H. Song).

costs than satellite remote sensing (Migliavacca et al., 2011; Julitta et al., 2014; Alberton et al., 2017; Lim et al., 2018). It can also provide imagery continuously over time and it is rarely obscured by clouds, and robust to variations in illumination conditions (Sonntag et al., 2012). The camera can track phenological transition dates (PTDs), such as leaf emergence, leaf discoloration, senescence, and green-up of vegetation with high temporal resolution (e.g., every 30 min, if desired) and obtain ecological information of the phenological responses (Ide and Oguma, 2010). Not only can the images provide the qualitative visual record but the quantitative value of colour indices also allows researchers to detect the changing phenological patterns (Richardson et al., 2007; Ide and Oguma, 2010; Zhao et al., 2012; Nagai et al., 2013b).

Measurements of carbon dioxide (CO<sub>2</sub>) exchange with continuous tower-based eddy-covariance (EC) methods between the atmosphere and vegetation cover are performed around the world (Reichstein et al., 2010). Moreover, digital cameras are widely used in CO<sub>2</sub> tower flux monitoring sites to interpret the seasonal variability of GPP (Richardson et al., 2007, 2013; Ahrends et al., 2008, 2009; Westergaard-Nielsen et al., 2013). The digital numbers of the colour indices are correlated with those in tower flux-based GPP (Ahrends et al., 2009; Richardson et al., 2009; Ide et al., 2011; Sonntag et al., 2011) and can be used to estimate the temporal and spatial distributions of photosynthetic productivity (Baldocchi et al., 2005; Saitoh et al., 2012). Additionally, the phenological variation influences the productivity and growth (carbon cycle) of an ecosystem (Richardson et al., 2013). A previous study focused on the carbon exchanges and climate sensitivity of carbon fluxes (GPP), ecosystem respiration (Reco) and net ecosystem carbon exchange (NEE) (Fei et al., 2018). However, there is a gap in the correlation between the canopy phenological variations and GPP in a savanna ecosystem on the regional scale.

Savannas are a key biome for terrestrial atmospheric carbon uptake via GPP and account for a quarter of the global GPP each year (Grace et al., 2006). Fei et al. (2017) highlighted that savanna ecosystems would be more sensitive to global climate changes in temperature and precipitation than forest ecosystems and suggested that their global carbon exchange should be monitored. Due to the large extent and spatial variation of savannas, satellite remote sensing was used to examine the interactions of savanna phenology with productivity (Broich et al., 2015) and determine its phenological variability from the landscape to the global scale (Ma et al., 2013, 2014). Although most of the researchers have investigated the seasonal change and interannual variation of the GPP of savanna vegetation, few studies have analysed the variation in patterns between GPP and phenological events of savanna ecosystems (Jin et al., 2013; Ma et al., 2013). In China, savanna ecosystems occur on areas in the Yunnan, Guizhou and Sichuan valleys, north-western Hainan, southern Taiwan, and the coastal hills of Guangdong. The study site of Yuanjiang savanna is a unique site characterized by a hot, dry climate that represents a type of Chinese savanna ecosystem (Editorial Committee for Vegetation of Yunnan, 1987). Due to the large extent and spatial variation of savannas, satellite remote sensing provides a useful tool (Broich et al., 2015) for examin-

ing the interactions of savanna phenology with productivity. On the regional scale, digital camera images are more suitable for assessing specific sites and species. The trees played an essential role in carbon uptake in the savanna, and this study examined how the canopy phenology and productivity responded to environmental constraints (average air temperature (air T), soil temperature (soil T), total precipitation (P), relative humidity (RH) and global radiation (Q)) in savanna ecosystems from 2014 to 2016. The pattern of phenology changes based on digital camera-based colour indices values were quantified by using visual estimates based on imagery (Ahrends et al., 2009) and used to investigate the correlation with productivity. The key questions to be answered were as follows: Can digital camera imagery be used to assess the variations of annual canopy development and ecosystem productivity of a savanna ecosystem? Can camera-derived colour indices of dominant tree species be used to analyze the relationship between the canopy phenology and productivity of the Yuanjiang savanna ecosystem? Can the effects of environmental constraints on canopy phenological variations and GPP in the savanna ecosystem be assessed? The combination of digital cameras with EC instrumentation reveals the relationship between the canopy phenology and the productivity. This paper aimed to determine the utility of colour indices derived from digital repeat photography for monitoring the annual canopy development and ecosystem productivity at savanna site, quantify the effect of the relationship between the canopy phenology and productivity on seasonal and growing season lengths, and examine the variability and changes in environmental factors, canopy phenology and GPP of a savanna ecosystem.

## 2. Materials and Methods

### 2.1. Study Site

The Yuanjiang savanna is located at 23°28'25.93"N, 102°10'38.76"E and 553 m a.s.l. in Yuanjiang Nature Reserve in Yunnan Province, Southwest China (Figure 1). The trees comprise dry-season deciduous species of small trees, shrubs, and herbs. They mainly consist of the dominant trees, namely *Lannea coromandelica*, *Polyalthia suberosa*, *Diospyros yunnanensis* and similar species; the dominant shrubs, which are *Vitex negundo* f. *laxipaniculata*, *Campylotropis delavayi*, *Woodfordia fruticosa*, *Euphorbia royleana*, *Jasminum nudiflorum* and *Taraxacum depauperata* and the dominant herbaceous species, namely *Heteropogon contortus* and *Bothriochloa pertusa*. These species have relatively small leaves with thick cuticles and smooth or waxy leaf surfaces to adapt to the region's high temperature and low rainfall (Fei et al., 2017). The climate is dry and hot with a mean annual temperature of 24.0 °C, and mean annual precipitation of 786.6 mm, with 81.0% of the total precipitation occurring during the rainy season (May to October). The soil is shallow (~ 35 cm in depth) and consists of approximately 65% gravel.

### 2.2. Digital Camera Setting

A digital camera (Ricoh Caplio R4) with a weatherproof enclosure was mounted at a height of 13 m above ground and

facing northwest on the 13.9 m high flux tower (Figure 2). The digital camera was installed on the flux tower in a fixed position with a 20-degree angle to overlook the canopies and capture images at a given time interval. The images were taken every 1.5 hours and stored in JPEG format (3,072 × 2,304 pixels). The camera was operated with the automated white balance adjustment to eliminate unwanted colour casts. The selected images were taken from 11:30 am to 1:00 pm to minimize the illumination angle (Ahrends et al., 2008; Ide and Oguma, 2010; Saitoh et al., 2012). Moreover, imaging requires clear-sky conditions, which provides the best format for monitoring canopy phenology (Sonntag et al., 2012). The images taken in rainy or dark conditions were excluded and one image per day with the best quality of R, G, and B was selected.

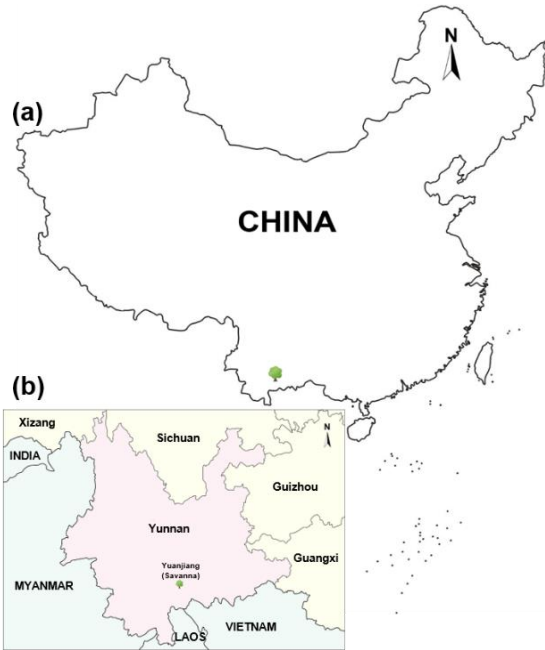


**Figure 1.** Location of the study site in China (a) Map of China (GS (2016) 1550); and (b) Map of Yunnan (GS (2019) 3266) (data source <http://bzdt.ch.mnr.gov.cn/>).

The three squared regions of interest (ROIs), namely ROI-1 for a prominent large tree canopy in focus, ROI-2 for a distant canopy behind the main tree to study the effect of distance, and ROI-3 for a background forest were set to measure a heterogeneous area and to study the effect of the atmospheric disturbance from one image that was valid for each image throughout the monitoring period (Figure 2c). The observation period in Yuanjiang lasted from 1 January 2014 to 31 December 2016. This study aimed to evaluate three PTDs: the start of the growing season (SGS) when leaves begin to appear or turn upwards during the day in the green up, the start of leaf senescence (SLS), when leaves begin to change color or the visible leaf coloring begins; and end of leaf senescence (ELS), when the tree is leafless. These events are commonly used in remote sensing and phenological studies (Ahrends et al., 2009; Zhao et al., 2012). The growing season length (GSL) was defined as the hydrolog-

ical year (the duration between the SGS and the ELS) (Luo et al., 2018).

### 2.3. Data Processing

R software (R Core Team, 2017) was used to analyse the images. In the images, the strength of green relative to the total RGB was used to detect the foliage phenology (Ahrends et al., 2008). The digital number of the R, G, and B channels of the fixed ROIs was extracted and the strength of each RGB colour channel ( $S_{red}$ ,  $S_{green}$ , and  $S_{blue}$ ) was calculated as follows (Gillespie et al., 1987):

$$S_{red} = R / (R + G + B) \quad (1)$$

$$S_{green} = G / (R + G + B) \quad (2)$$

$$S_{blue} = B / (R + G + B) \quad (3)$$

where  $R$  is the red digital values,  $G$  is the green digital values and  $B$  is the blue digital values of each colour channel from image files.

*HUE* is one part of the Hue Saturation Lightness colour scheme. The *HUE* values were calculated as follows (Joblove and Greenberg, 1978; Nagai et al., 2016):

$$HUE = [(B - R) / (I_{max} - I_{min})] \times 60 + 120, \text{ if } G = I_{max} \quad (4)$$

$$HUE = [(R - G) / (I_{max} - I_{min})] \times 60 + 240, \text{ if } B = I_{max} \quad (5)$$

$$HUE = [(G - B) / (I_{max} - I_{min})] \times 60 + 360, \text{ if } G < B \quad (6)$$

$$HUE = [(G - B) / (I_{max} - I_{min})] \times 60 \text{ otherwise} \quad (7)$$

where  $I_{max}$  is the maximum value of  $R$ ,  $G$ , and  $B$ ; and  $I_{min}$  is the minimum value of  $R$ ,  $G$ , and  $B$ .

The *GEI* (Woebbecke et al., 1995) is widely used to describe canopy greenness and is defined as follows:

$$GEI = (G - R) + (G - B) = 2G - (R + B) \quad (8)$$

A new related index, the vegetation contrast index (*VCI*), was calculated in each pixel as follows (Zhang et al., 2018):

$$VCI = \frac{G}{(R + B)} \quad (9)$$

The *VCI* contrasts the green channel relative to the sum of the red and blue channels. The *VCI* is a nonlinear transformation of the green chromatic coordinate resulting in a higher dynamic range for the *VCI* relative to the  $S_{green}$ .

### 2.4. Eddy Flux Data and Environmental Factors

The air temperature and the relative humidity were mea-

**Table 1.** Phenological Transition Dates – Start of The Growing Season (SGS), Start of Leaf Senescence (SLS) and End of Leaf Senescence (ELS) and Phenological Period – Growing Season Length (GSL) of Different Regions of Interest (ROIs) from 2014 to 2016

Year	ROI-1				ROI-2				ROI-3			
	SGS	SLS	ELS	GSL	SGS	SLS	ELS	GSL	SGS	SLS	ELS	GSL
2014 (DOY)	120	279	345	225	120	279	345	225	120	279	345	225
2015 (DOY)	147	303	345	198	147	303	345	198	147	303	345	198
2016 (DOY)	120	279	345	225	120	279	345	225	120	279	345	225

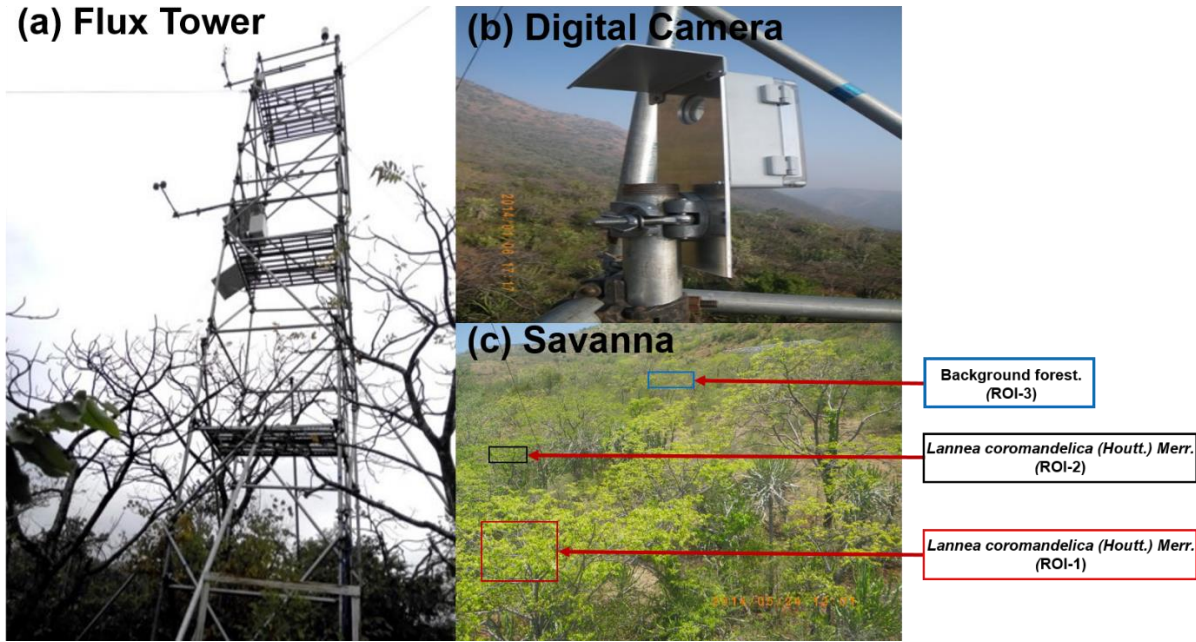


**Figure 2.** Digital camera setting. (a) Flux tower, (b) Digital camera, (c) Savanna’s sample image and regions of interest (ROIs), namely ROI-1, a prominent large tree canopy; ROI-2, a distant canopy behind the main tree; and ROI-3, the background forest, 24 May 2014 on Yuanjiang savanna.

sured using a temperature sensor (HMP45C®, Vaisala, Helsinki, Finland) installed at a height of 13 m above ground on the 13.9 m high flux tower. In addition, precipitation was measured using rain gauges (Rain Gauge 52203®, Young Co., Traverse City, MI, USA) installed at the top of the flux tower. Global radiation was measured using radiation sensors (CNR-1/CM11®, Kipp & Zonen, Delft, Netherlands) in terms of downward, upward and short- and long-wave radiation. The radiation sensor was installed at a height of 8.5 m above ground using a horizontal pole fixed within 3 m of the flux tower. Soil temperature at 10 cm depth was measured using a frequency domain reflectometer (105T/107\_L, Campbell Scientific Inc., Logan, UT, USA). All the environmental data were collected using a CR1000 data logger (Campbell Scientific, Logan, UT, USA), with the time interval set at every 30 min. Due to machine error, the data related to air temperature, global radiation, relative humidity and soil temperature for the period 15 May to 31 December 2015 was missing. The EC system consisted of a triaxial sonic anemometer (CSAT3, Campbell Scientific Inc., Logan, UT, USA) and a high-frequency open-path CO<sub>2</sub>/H<sub>2</sub>O infrared gas analyser (Li-7500, Li-Cor Inc., USA) installed on the flux tower at a

height of 13.9 m above ground. The detailed of the installation system at this station have been published previously (Fei et al., 2018).

Forest ecosystem productivity (*GPP*) was calculated as follows (Gilmanov et al., 2007; Zhou et al., 2019):

$$GPP = R_{eco} + (-NEE) \quad (10)$$

$$R_{eco} = R_{eco,ref} \times e^{E_0 \left( \frac{1}{T_{ref} - T_0} - \frac{1}{T - T_0} \right)} \quad (11)$$

where  $R_{eco,ref}$  is the reference ecosystem respiration at the reference temperature ( $T_{ref}$ ; here, 283.15 K),  $E_0$  is the fitted parameter,  $T_0$  is a constant set to 227.13 K, and  $T$  is the measured soil temperature at 10 cm in this study.

The *NEE* consists of the turbulent eddy flux ( $F_c$ ) and the storage flux ( $F_s$ ) as follows (Hollinger et al., 1994):

$$NEE = F_c + F_s = \overline{\rho w'c'} + \frac{\Delta c}{\Delta t} \quad (12)$$

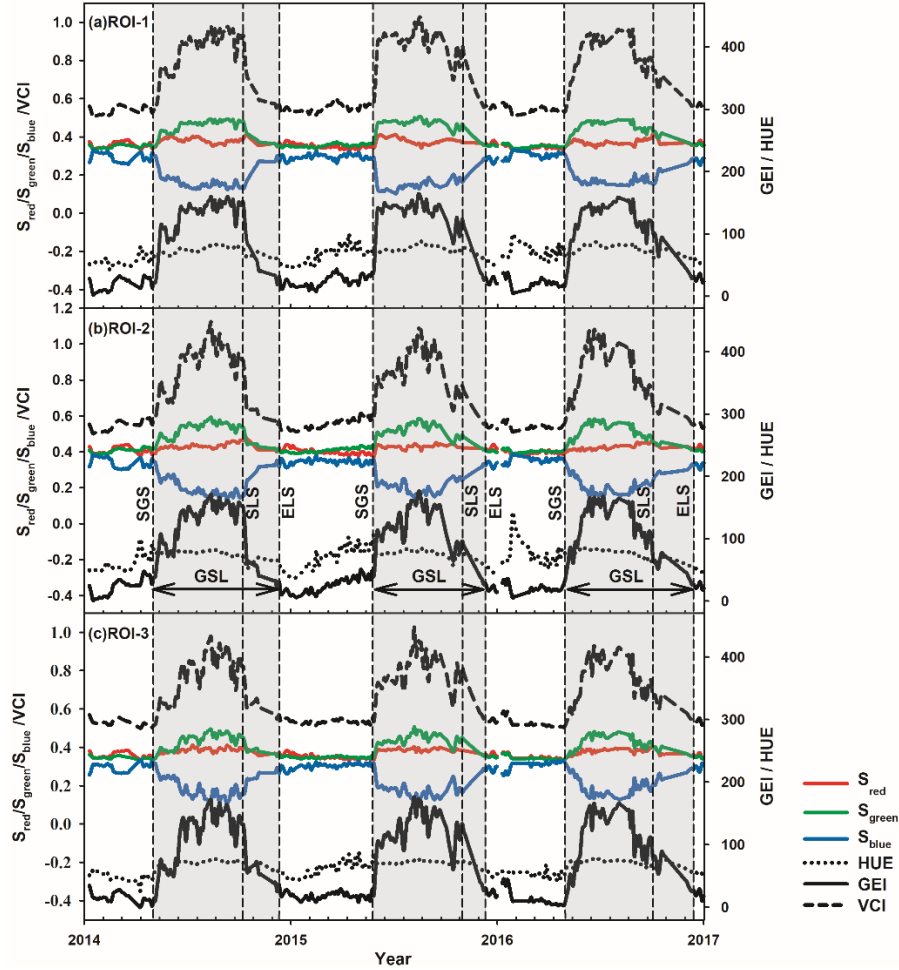


**Figure 3.** Conceptual figure of the seasonal dynamic of the colour indices ( $S_{red}$ : Strength of red;  $S_{green}$ : Strength of green,  $S_{blue}$ : Strength of blue,  $HUE$ ,  $GEI$ : Green excess index and  $VCI$ : vegetation contrast index) and their phenological transition dates (PTDs) for dominant species in (a) ROI-1, (b) ROI-2, and (c) ROI-3, the background forest, from 2014 to 2016. The vertical dashed lines represent the phenological events and the corresponding names are shown (SGS: start of the growing season; SLS: start of leaf senescence; ELS: end of leaf senescence). The time interval between SGS and ELS is defined as GSL (growing season length), which is indicated in the figure with a grey rectangle. A detailed description of PTDs is provided in Table 1.

where  $F_c$  represents the turbulent eddy flux transported above the height of the EC system and the atmosphere and  $F_s$  indicates the storage flux under the plane of the EC system and the ground surface. A single-point method was applied to measure  $F_s$  at the measurement height ( $z_r$ ) of the fluxes. In addition,  $\rho$ ,  $w$ , and  $c$  represent the air density, vertical wind velocity, and target scalar concentration, respectively; the primes denote fluctuations from the average, and the overbar signifies the average taken over a given time (30 minutes in this case).  $\Delta c$  is the variation over a 30-min period at height  $z_r$ ,  $z_r$  is the height of the EC system, and  $\Delta t$  is the time interval (1,800 s in this case).

### 2.5. Data Analysis

The colour indices from digital camera images:  $S_{red}$ ,  $S_{green}$ ,  $S_{blue}$ ,  $HUE$ ,  $GEI$  and  $VCI$ , were computed. Subsequently, the PTDs were extracted by visual inspection using the canopy surface images (Ahrends et al., 2008; Ahrends et al., 2009; Inoue

et al., 2014; Nagai et al., 2014; Wingate et al., 2015) and their uncertainty was assessed by extracting PTDs repeatedly (18 times) from digital camera set time series by combining a random noise (Filippa et al., 2016), the data of low visibility images were excluded. A three-day moving window, yielding up to 122 observations each year, (Sonntag et al., 2012; Toomey et al., 2015) was applied to minimize the impact of variation in lighting and weather conditions. By calculating values over a three-day window, the result smoothed out noise in the data when change occurred in the colour indices time series (Browning et al., 2017). Regression analysis was performed to evaluate the consistency between colour indices and GPP. Regression is a long established statistical tool that is widely used in phenological research to detect changes in the dates of phenological events and to relate the date of phenological events to environmental conditions. Correlation coefficients and significance levels were used to estimate the relationship between two random variables. A linear model was employed to analyse the relation-

ship between phenological events (SGS) and environmental factors (air T, total P, RH, Q and soil T), and multiple linear models were used to analyse the relationship between phenological events (SGS) and environmental factors (air T, Q and soil T) from February to April in 2014 and 2016. The linear models were also used to analyse the relationship between phenological events (SGS) and colour indices (*GEI*) and productivity (*GPP*) throughout the years, the relationship between colour indices (*GEI*) and productivity (*GPP*) during the growing season length, and the monthly relationship between the *GPP* and colour indices (*S<sub>green</sub>*, *HUE*, *GEI* and *VCI*). A significance level of  $p < 0.05$  was considered as statistically significant between the groups. Statistical analysis was performed using SigmaPlot for Windows (Systat Software, version 12.5, Chicago, IL, USA).

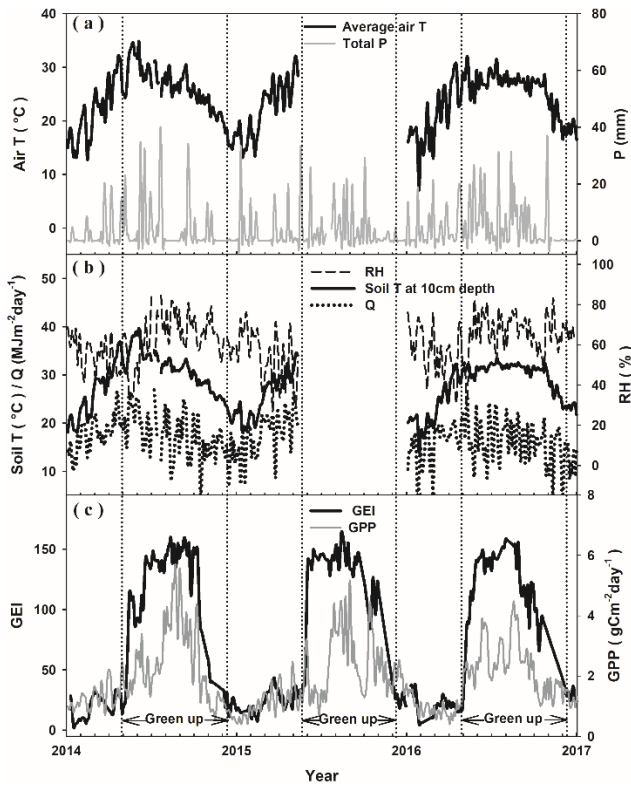


**Figure 4.** Seasonal variations in (a) air temperature (Air T) and precipitation (P); (b) soil temperature at 10 cm depth (soil T), global solar radiation (Q), and relative humidity (RH); and (c) green excess index (*GEI*) and gross primary productivity (*GPP*). Dotted lines indicate the start and end of the green-up period determined from the *GEI*.

### 3. Results and Discussion

#### 3.1. Seasonal Patterns and Variations in Colour Indices

The red, green, and blue values extracted from images for different ROIs are shown in Figure 2c. Digital camera-based colour indices are considered useful for monitoring the phenological dynamics of many biomes, and researchers have used different colour indices to carry out quantitative analyses (Nagai et

al., 2013b; Nagai et al., 2014, 2016). The inverted U-shaped seasonal pattern for the colour indices (*S<sub>green</sub>*, *GEI* and *VCI*) except *S<sub>blue</sub>* found in Figure 3. The *S<sub>green</sub>*, *GEI* and *VCI* values increased sharply when leaf sprouting started. Thereafter, a slight fluctuation in the pattern was observed during the wet period (from May to November) until a dramatic decrease associated with the dry period (from December to April) was observed. The *S<sub>blue</sub>* values decreased slightly during the wet period but increased again in the dry period. The *S<sub>red</sub>* values were less variable than the *S<sub>blue</sub>* and *S<sub>green</sub>* values. The brightness of the blue channel responded to spring green-up and was more sensitive to changes in the quality of incident radiation (Richardson et al., 2007). In our study site, the *S<sub>green</sub>* value increased and the *S<sub>blue</sub>* value decreased at the start of the leaf development period. With ongoing leaf senescence, *S<sub>blue</sub>* increased rapidly, causing a decrease in *S<sub>green</sub>*. The comparison of several colour indices showed that the *HUE* value provided a more robust metric than the other indices (Mizunuma et al., 2011, 2014), while the redness index was better for estimating leaf senescence and the greenness index was better for estimating leaf development events (Zhao et al., 2012). In this study site, the *S<sub>red</sub>* and *HUE* values did not show an evident pattern associated with the phenological events. The *S<sub>green</sub>*, *VCI* and *GEI* showed the seasonal change in the phenological pattern distinctly and can represent the phenological variations in the savanna ecosystem. Among the colour indices, the *GEI* is suitable for a savanna ecosystem.

The colour index patterns of different ROIs, namely ROI-1 (Figure 3a), ROI-2 (Figure 3b) and ROI-3 (Figure 3c), were very similar throughout the study period. The SGS, SLS, ELS and GSL were also the same. Therefore, there were no external effects of environmental conditions, especially distance from the objects, on the digital camera. The response of the different ROIs to climatic factors was also the same in this study site. Therefore, the colour index patterns of a small ROI derived from the dominant trees could represent the whole study area.

#### 3.2. Dynamics of Phenological Events

The phenological shifts can be recognized as a sensitive indicator of the ecological impacts of climate change (Walther et al., 2002). The phenological transition dates the SGS, SLS, ELS and GSL based on digital camera-derived data sets were investigated in this study. The growth of dominant species commenced in the SGS on the 120<sup>th</sup>, 147<sup>th</sup> and 120<sup>th</sup> day of the year in 2014, 2015, and 2016, respectively, with the earliest SGS in 2014 and 2016, and the latest in 2015. The SLS occurred earlier in 2014 and 2016 (279<sup>th</sup> day) and the later in 2015 (303<sup>rd</sup> day), although the ELS occurred on the same day (345<sup>th</sup> day).

At the ecosystem level, the dates of leaf out and senescence in plants influence the GSL (Dragoni et al., 2011; Keenan et al., 2014). The growing season extended to the 225<sup>th</sup> day in 2014 and 2016, and the 198<sup>th</sup> day in 2015 (Figure 3). Detailed information on the phenological events of different regions of interest is shown in Table 1. The long-term study of the phenological events shows that leaf-out dates vary interannually and are essential for understanding the environmental cues of leaf-out (Tang et al., 2016). The leaf-out data across species, ecosys-

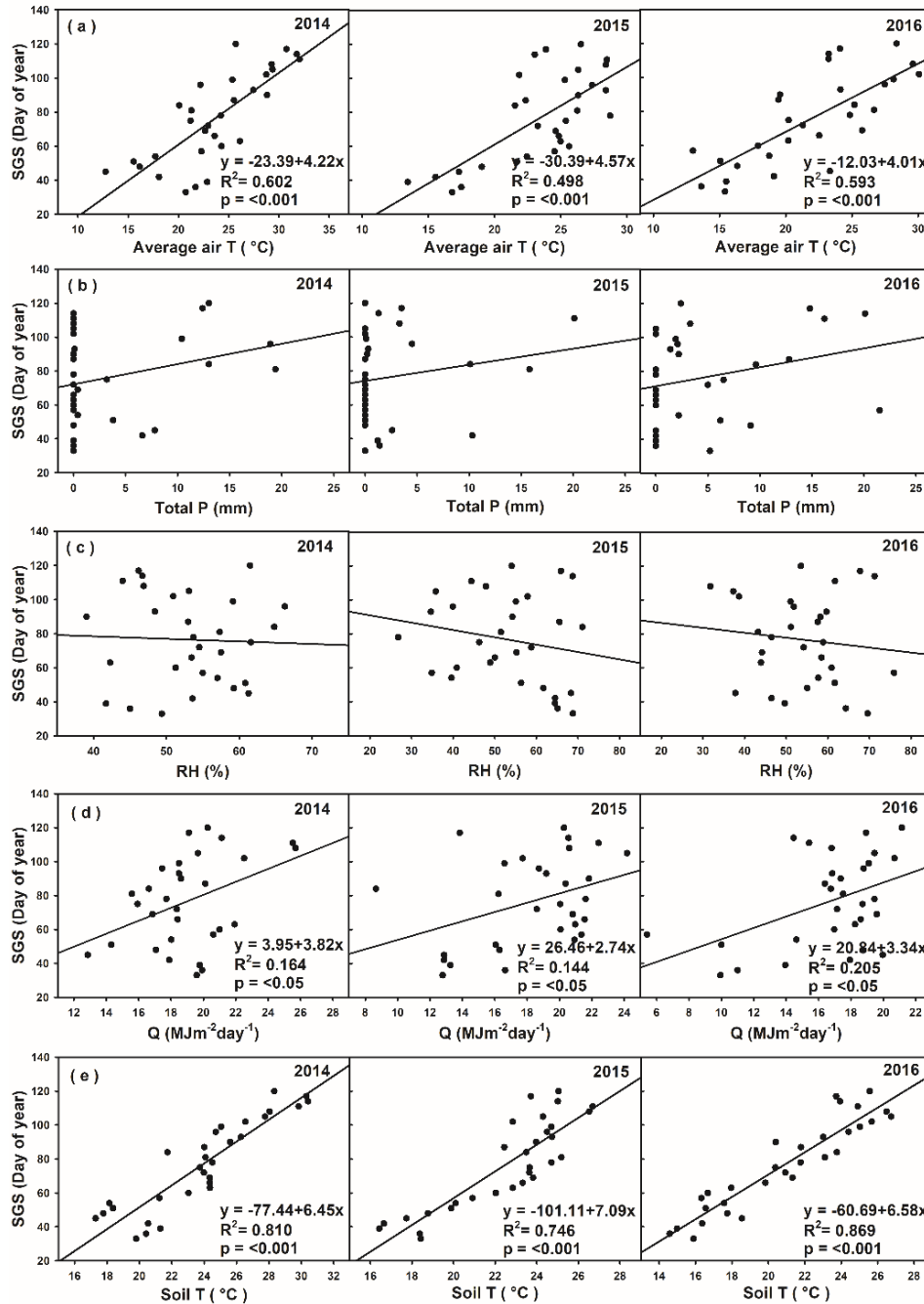


**Figure 5.** Relationships between phenological events (start of the growing season: SGS) and environmental factors from 2014 to 2016. The regression lines were calculated when those relationships were significant ( $p < 0.05$ ). (a) SGS and average air temperature (average air T), (b) SGS and total precipitation (total P), (c) SGS and relative humidity (RH), (d) SGS and global solar radiation (Q), and (e) SGS and soil temperature (soil T) from February to April in 2014 and 2016 to SGS, respectively.

tems, and biomes throughout the years are important to investigate the responses of phenology to environmental change (Tang et al., 2016). The yearly variations in daily mean air temperatures affected the timing of the start of leaf expansion and end of leaf fall (Nagai et al., 2013a; Inoue et al., 2014). However, our results showed that the phenological trends were not

continuous within the study period. Changes in temperature affect the date of phenology changes (Dai et al., 2014; Güsewell et al., 2017). The increasing temperature caused advances in leaf flushing and delay in leaf senescence (Vitasse et al., 2009). The advanced SGS increases vegetation productivity with the increasing trends in seasonal and growing season temperatures

(Kang et al., 2016). The SGS trend indicated a delay in 2015 which suggested the occurrence of the impact of climate change.

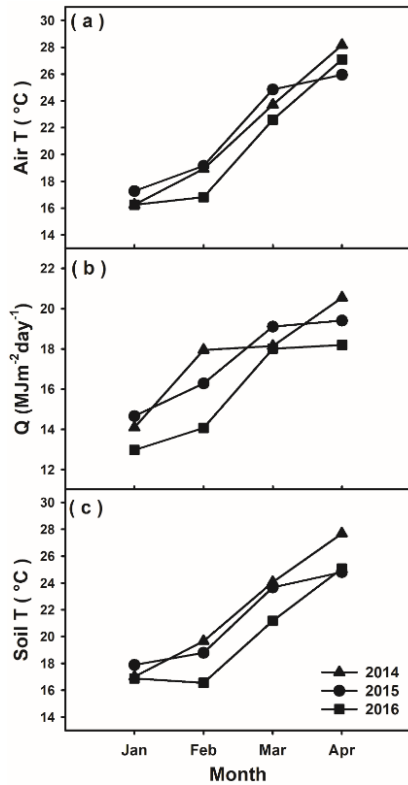


**Figure 6.** Variation in the monthly mean values of environmental factors. (a) Average air temperature (b) Global radiation and (c) Soil temperature at 10 cm depth in the period before the start of the growing season (SGS) from January to April from 2014 to 2016.

Moreover, the investigation of the year-to-year variations and long-term trends in the timing of the phenological transition dates is important since they affect spatial and temporal variations in water, heat and carbon cycles (Nagai et al., 2013a; Inoue et al., 2014). The SGS in 2015 was delayed compared with that in 2014 and 2016 but no the difference was found in the time of ELS due to the effect of air temperature. The air temperature effect on the phenological sensitivity of the start of leaf expansion was lower than the end of leaf fall among deciduous broad-leaved species (Inoue et al., 2014). In our results, the air temperature had a significant relationship ( $p < 0.001$ ) with the SGS throughout the year, but the regression coefficients in 2014 and 2016 were higher than in 2015 (Figure 5a). This indicates the delayed effect of the phenological sensitivity of the timing of SGS in 2015. The warmer temperatures corresponded to an earlier SGS, increased *GPP*, and an increased carbon sink (Vitasse et al., 2009; Kang et al., 2016). The annual *GPP* of terrestrial ecosystems is influenced by the plant growing period (Baldocchi et al., 2005; Richardson et al., 2010). The GSL has a strong effect on the ecosystem functioning and tree productivity (Kramer et al., 2000; Picard et al., 2005). In our study, the

GSL in 2015 was shorter than those in the other years, which had an effect on productivity.

### 3.3. Environmental Factors that Control Phenology and Productivity

Digital images of tree canopies have been analysed to gain an understanding of how forest phenology responds to climate change. Differences in the patterns of annual phenology on the scale of the savanna ecosystem occurred because of differences in the course of environmental factors each year. Comparisons between environmental values and interpolated phenological events from the digital camera images yielded the precise pattern of environmental data sets, namely air temperature, precipitation, relative humidity, global radiation and soil temperature (Figure 4). The timing of phenological patterns and the onset and offset of greenness, are strongly influenced by environmental conditions. The annual date of the SGS was associated with the pattern of air T, Q and soil T throughout the year and a high correlation coefficient of  $p < 0.001$  with air T and soil T was observed, while Q had a correlation coefficient of  $p < 0.05$ . There was no significant correlation with the pattern of P and RH (Figure 5). There were multiple relationships between the SGS and environmental factors (air T, Q, and soil T) in 2014 ( $R^2 = 0.848$ ,  $p < 0.001$ ), 2015 ( $R^2 = 0.788$ ,  $p < 0.001$ ) and 2016 ( $R^2 = 0.919$ ,  $p < 0.001$ ). Among them, SGS had a significant relationship ( $p < 0.05$ ) with soil T in 2016. The interannual variations in green-up dates were strongly correlated with the local spring temperature (Ide and Oguma, 2010). The pattern of global radiation (Q) can investigate the timing of leaf flush (Do et al., 2005) and the productivity of tropical savanna in the wet season (Moore et al., 2018). Our results showed that the SGS was significantly correlated with the air temperature, global radiation and soil temperature throughout the year.

The monthly mean values of air T and soil T increased steadily from January to April until the SGS in 2014 and 2016. Furthermore, the trend showed a steady increase from January to March followed by a decline in April in 2015. A distinct trend in global radiation was not observed within the studied period (Figure 6). The average air temperature was significantly related to the SGS (Du et al., 2014; Inoue et al., 2014). In addition, the green-up period was related to soil temperature (Snyder et al., 2016). The average air and soil temperatures in 2014 and 2016 increased steadily until the SGS, although the same change did not occur for global radiation. The increasing temperature caused the advance in the timing of the SLS, which was earlier in 2014 and 2016 than in 2015. The effect of earlier spring green-up caused soil water depletion that enhanced drought in some cases (White and Nemani, 2003). Therefore, the advance in green-up in 2014 and 2016 indicates the occurrence of soil water depletion.

### 3.4. Relationship between GEI and GPP during the GSL

The SGS was significantly correlated with the colour index (GEI) in 2014 ( $p < 0.05$ ) but not in 2015 and 2016. The SGS was significantly correlated ( $p < 0.05$ ) with productivity (GPP)

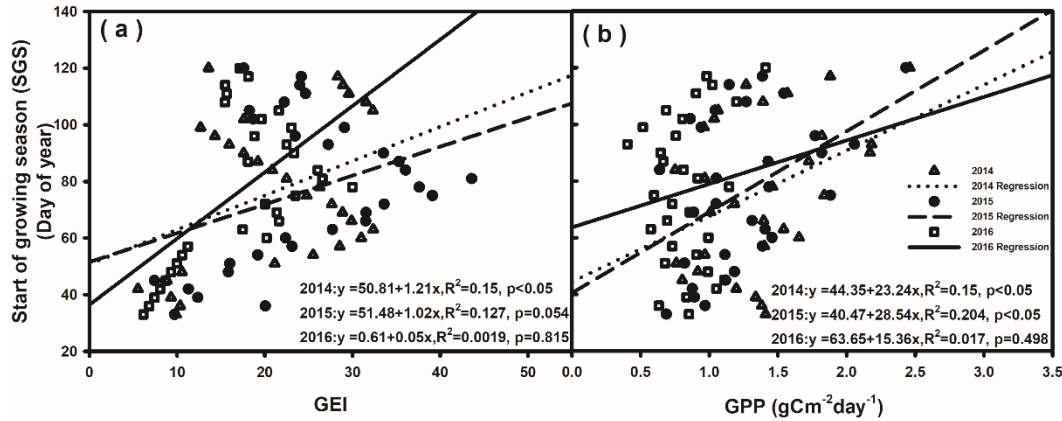


**Figure 7.** Relationship between phenological event (start of the growing season: SGS) and colour indices (green excess index: *GEI*) and productivity (gross primary production: *GPP*): (a) SGS and *GEI* and (b) SGS and *GPP* from 2014 to 2016.

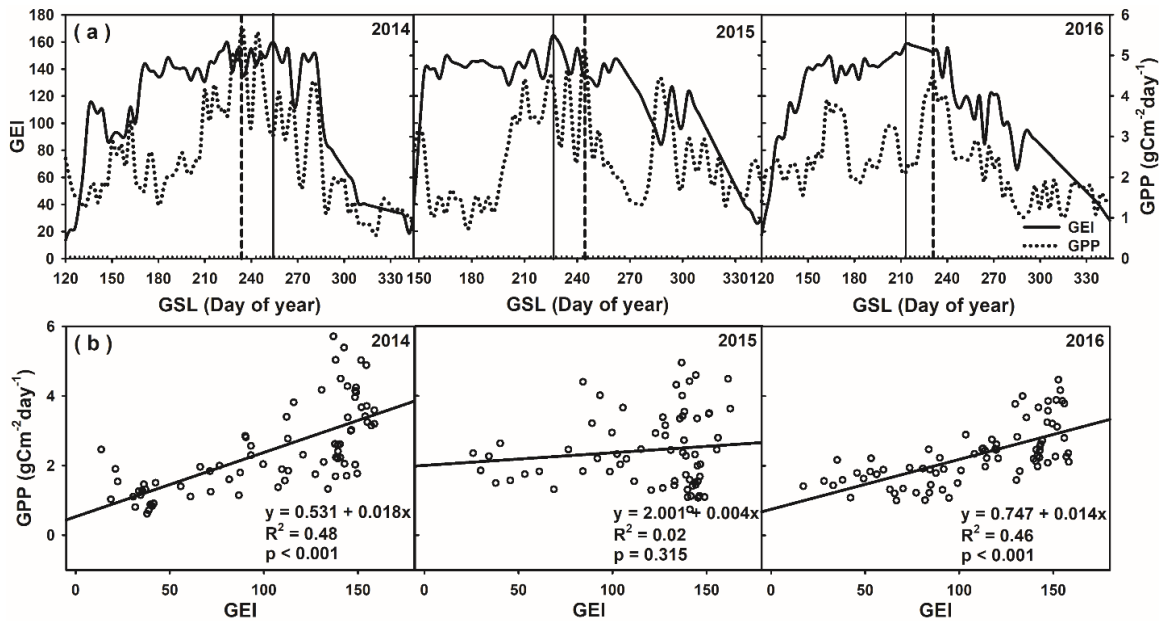


**Figure 8.** (a) Variations in phenological event (green excess index: *GEI*) and productivity (*GPP*). The vertical black line represents the peak of *GEI* and the dotted line represents the peak of *GPP*. (b) Relationship between *GEI* and *GPP* during the growing season length from 2014 to 2016.

in 2014 and 2015 but not in 2016 (Figure 7). Although an increase in the green-based index was evident with the onset of leaves, the sharp increase was not consistent with the gradual increase of daily *GPP* from the carbon flux measurements. The pattern of canopy greenness might be indicative of photosynthetically active green leaves. *GPP* was also strongly correlated with canopy greenness (Richardson et al., 2009; Migliavacca et al., 2011; Toomey et al., 2015). Moreover, the *GSL* affected the productivity (Churkina et al., 2005). Additionally, the day of year (DOY) of the maximum *GEI* value was assessed to determine the approximate date when leaf-out processes had finished. Maximum *GEI* values represent maximum canopy closure within the ROI. When the analysis focused on the *GSL*, the peaks of the *GEI* were observed later than the peaks of daily *GPP* in 2014

and earlier than the peaks of daily *GPP* in 2015 and 2016. The peak value of the *GEI* and *GPP* events occurred on DOY 255 and DOY 234 in 2014, DOY 228 and DOY 243 in 2015 and DOY 213 and DOY 231 in 2016, respectively (Figure 8a). However, strong significant correlation coefficients were found between *GPP* and *GEI* in 2014 ( $p < 0.001$ ,  $R^2 = 0.48$ ) and 2016 ( $p < 0.001$ ,  $R^2 = 0.46$ ) but not in 2015 ( $p = 0.315$ ,  $R^2 = 0.02$ ) (Figure 8b). The relationship between the three camera-based indices (*GEI*,  $S_{green}$  and *HUE*) and *GPP* appeared to have different characteristics at different phenological stages (Saitoh et al., 2012). Among them, a strongly significant relationship between *GPP* and *GEI* was found during the period of the *GSL* in 2014 and 2016. Therefore, the *GEI* was useful for investigating the forest ecosystem productivity in the savanna ecosystem.

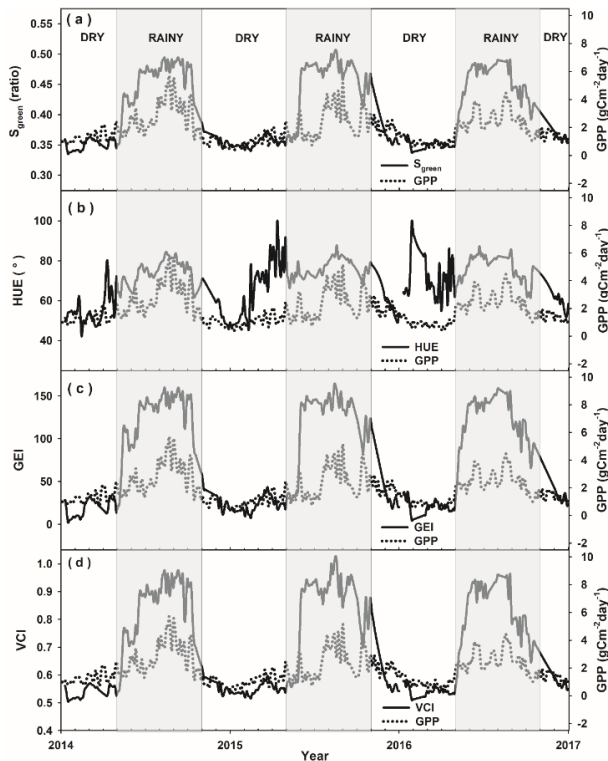


**Figure 9.** Seasonal variations in camera-based indices (Strength of green:  $S_{green}$ ;  $HUE$ ; green excess index:  $GEI$ , and vegetation contrast index:  $VCI$ ) and gross primary productivity ( $GPP$ ) (a)  $S_{green}$  and  $GPP$ , (b)  $HUE$  and  $GPP$ , (c)  $GEI$  and  $GPP$ , and (d)  $VCI$  and  $GPP$ .

When the canopy greenness was used as a predictor of  $GPP$ , there were some limitations: temperature had a negative effect and precipitation had a positive effect on the  $GPP$  (Fei et al., 2018). Sonntag et al. (2011) showed a lag time between colour indices and  $GPP$  indicating differences in structure, functioning and greenness in a grassland ecosystem. Peak values of colour indices were caused by the seasonal variation in foliage pigments (Sims and Gamon, 2002). Higher photosynthetic activity was related to the peak value of  $GPP$  (Kikuzawa, 1991; Arndal et al., 2009) and delayed photosynthetic activity was related to the peak value of colour indices (Westergaard-Nielsen et al., 2013). Although the comparison of the peak values of the color indices and  $GPP$  was observed in managed mixed forest and deciduous forest (Ahends et al., 2009; Mizunuma et al., 2013), Arctic tundra (Kim et al., 2012) and rubber plantation (Zhou et al., 2019), it was not found in any research in the savanna. When the study focused on the savanna, the results showed that the peak values of  $GPP$  occurred earlier than the  $GEI$  in 2014 and were delayed in 2015 and 2016. The earlier peak value of  $GPP$  indicates that earlier and higher photosynthetic activity occurred in 2014.

### 3.5. Seasonal Variation and Relationship between Colour Indices and Productivity

The seasonal variations in colour indices obtained from dif-

ferent ROIs, namely ROI-1, ROI-2 and ROI-3, showed similar patterns within our study site (Figure 3). Although a small ROI was chosen, it could represent the whole study area ecosystem because of the strong relationship of the seasonal dynamics between the colour indices and  $GPP$ . The relationship between the four camera-based indices ( $S_{green}$ ,  $HUE$ ,  $GEI$  and  $VCI$ ) and  $GPP$  appeared to have different characteristics at different phenological stages. The indices ( $S_{green}$ ,  $HUE$ ,  $GEI$  and  $VCI$ ) increased after leaf sprouting and greening-up began at the start of the rainy season, which preceded an increase in  $GPP$ . As the leaves started their coloration at the end of the rainy season, the indices declined significantly, which occurred later than the  $GPP$ . Thus, the seasonal variations in the phenology of the dominant trees captures by the camera-based indices were similar to the seasonal  $GPP$  variations (Figure 9).

The seasonal (dry and wet) and annual relationships between  $GPP$  and the camera-based colour indices ( $S_{green}$ ,  $HUE$ ,  $GEI$  and  $VCI$ ) were shown in Table 2. There was only a significant relationship ( $p < 0.05$ ) between  $GPP$  and  $S_{green}$ ,  $GEI$  and  $VCI$  in the dry season of 2016. A significant relationship ( $p < 0.05$ ) between  $GPP$  and  $HUE$  and  $VCI$  was found in the wet season of 2014 and between  $S_{green}$ ,  $HUE$ ,  $GEI$  and  $VCI$  in 2016. The annual pattern of the  $GPP$  was significantly correlated with  $S_{green}$ ,  $GEI$  and  $VCI$  throughout the year. A strongly significant relationship ( $p < 0.001$ ) was observed in 2014 and 2016, and a significant relationship ( $p < 0.05$ ) was observed in 2015. Moreover,  $HUE$  was strongly significantly correlated ( $p < 0.001$ ) with  $GPP$  only in 2014, but there was no significant relationship in 2015 and 2016 (Figure 10). The seasonal pattern in the  $GEI$  was correlated with the  $GPP$  of a forest (Richardson et al., 2009). This result showed that the annual variations in the three camera-based indices,  $S_{green}$ ,  $VCI$  and  $GEI$ , correspond to  $GPP$ , although this was not observed for  $HUE$ . Thus, the annual variations in colour indices derived from digital camera images were related to the productivity in a savanna ecosystem.

## 4. Conclusions

Determining the responses of forest phenology to environmental factors on regional scales is critical for investigating forest ecosystem productivity. This study assessed the use of colour index values derived from digital camera images to detect shifts in phenological events and  $GPP$ . The colour indices derived from the digital camera images represented the phenological variations in the savanna ecosystem. On the regional scale, digital camera images were useful and suitable for assessing the response of specific sites and species to environmental factors. The increasing air and soil temperatures caused the advance in green-up, which indicates the occurrence of soil water depletion. The delay in the phenological event (SGS) in 2015 indicates the occurrence of the impact of climate change. Furthermore, the shorter GSL in 2015 indicates the occurrence of the impact on productivity. The earlier peak values of  $GPP$  than  $GEI$  indicate the increase in photosynthetic activity in 2014. The annual phenological variations of the dominant trees from the camera-based indices could assess the productivity of the savanna. Phenological images could eventually be used as environmental data to

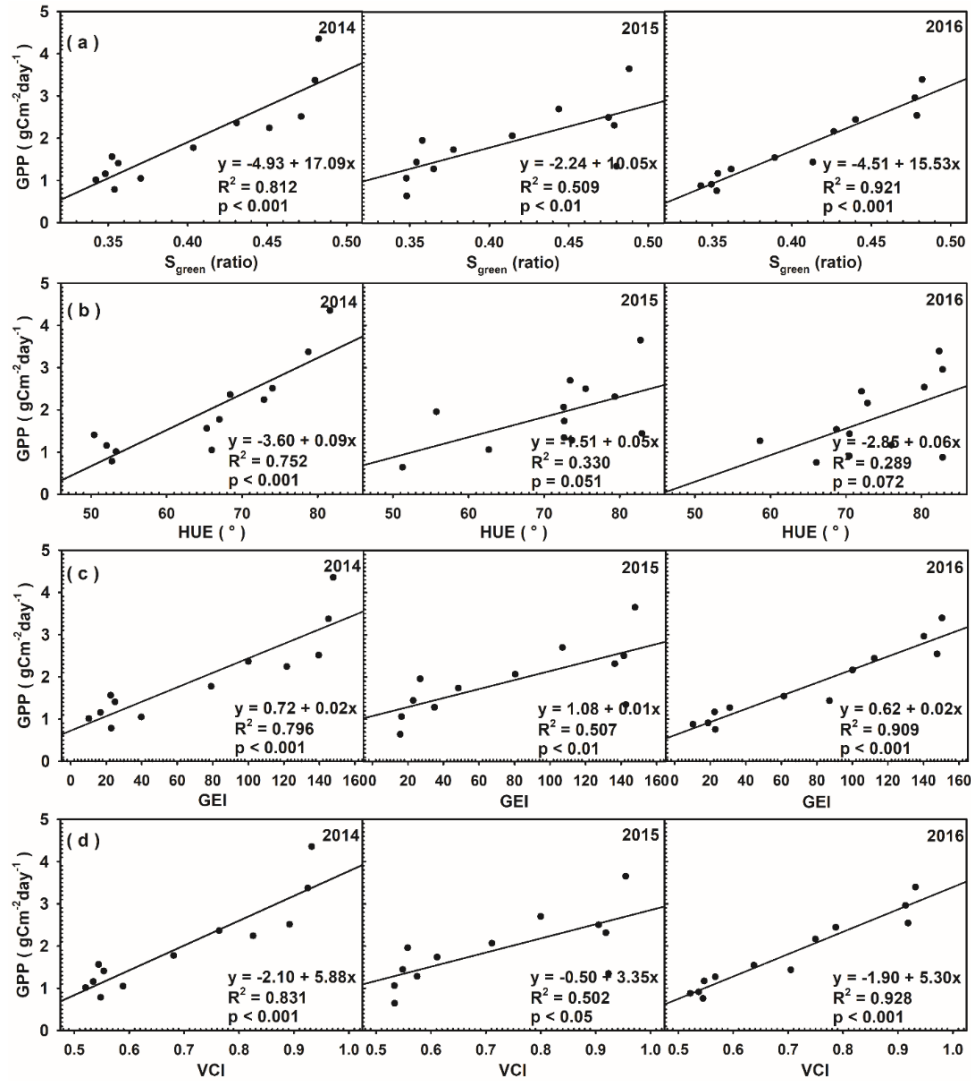


**Figure 10.** Monthly relationships between (a) *GPP* (gross primary production) and *S<sub>green</sub>* (strength of green), (b) *GPP* and *HUE*, (c) *GPP* and *GEI* (green excess index), and (d) *GPP* and *VCI* (vegetation contrast index) from 2014 to 2016.

**Table 2.** Seasonal Relationship between Productivity and Colour Indices (*S<sub>green</sub>* – Strength of Green, *HUE*, *GEI* – Green Excess Index, and *VCI* – Vegetation Contrast Index) from 2014 to 2016

Season	Variables	2014		2015		2016	
		<i>R</i> <sup>2</sup>	<i>p</i>	<i>R</i> <sup>2</sup>	<i>p</i>	<i>R</i> <sup>2</sup>	<i>p</i>
Dry	<i>GPP</i> & <i>S<sub>green</sub></i>	0.0001	0.987	0.479	0.128	0.760	<0.05
	<i>GPP</i> & <i>HUE</i>	0.0829	0.580	0.111	0.519	0.088	0.568
	<i>GPP</i> & <i>GEI</i>	0.0008	0.958	0.496	0.118	0.733	<0.05
	<i>GPP</i> & <i>VCI</i>	0.0002	0.977	0.467	0.134	0.759	<0.05
Wet	<i>GPP</i> & <i>S<sub>green</sub></i>	0.654	0.054	0.141	0.463	0.792	<0.05
	<i>GPP</i> & <i>HUE</i>	0.866	<0.01	0.621	0.063	0.738	<0.05
	<i>GPP</i> & <i>GEI</i>	0.622	0.062	0.130	0.483	0.791	<0.05
	<i>GPP</i> & <i>VCI</i>	0.669	<0.05	0.144	0.458	0.791	<0.05
Annual	<i>GPP</i> & <i>S<sub>green</sub></i>	0.812	<0.001	0.509	<0.01	0.921	<0.001
	<i>GPP</i> & <i>HUE</i>	0.752	<0.001	0.330	0.051	0.289	0.072
	<i>GPP</i> & <i>GEI</i>	0.796	<0.001	0.507	<0.01	0.909	<0.001
	<i>GPP</i> & <i>VCI</i>	0.830	<0.001	0.502	<0.05	0.928	<0.001

evaluate the sensitivity of tree phenology and productivity to environmental changes in the savanna. Moreover, the effect of environmental constraints on phenological dynamics in the savanna ecosystem is complex and needs to be addressed over a long-term periods.

**Acknowledgments.** This study was funded by CAS, Key Laboratory of Tropical Forest Ecology, Xishuangbanna Tropical Botanical Garden, Chinese Academy of Sciences, Xishuangbanna, China; the National Natural Science Foundation of China (31770528, 42075119, 41961144017, 41975147); the National Key Research and Development Program of China (2016YFC0502105); and the Chinese Academy of Sciences 135 project (2017XTBG-T01; 2017XTBG-F01). We also thank the Central Laboratory and Biogeochemistry Laboratory of Xishuangbanna Tropical Botanical Garden, Chinese Academy of Sciences. We would like to acknowledge the staff and technicians of Xishuangbanna Station. Finally, STZM thanks the Myanma Timber Enterprise of Myanmar for its encouragement.

## References

- Ahends, H.E., Etzold, S., Kutsch, W.L., Stoeckli, R., Bruegger, R., Jeanneret, F., Wanner, H., Buchmann, N. and Eugster, W. (2009). Tree phenology and carbon dioxide fluxes: Use of digital photography for process-based interpretation at the ecosystem scale. *Clim. Res.*, 39, 261-274. <https://doi.org/10.3354/cr00811>
- Ahrends, H.E., Brügger, R., Stöckli, R., Schenk, J., Michna, P., Jeanneret, F., Wanner, H. and Eugster, W. (2008). Quantitative phenological observations of a mixed beech forest in northern Switzerland with digital photography. *J. Geophys. Res-Bioge.*, 113, 1-11. <https://doi.org/10.1029/2007JG000650>
- Alberton, B., Torres, R.S., Cancian, L.F., Borges, B.D., Almeida, J., Mariano, G.C., dos Santos, J. and Morellato, L.P.C. (2017). Introducing digital cameras to monitor plant phenology in the tropics: applications for conservation. *Perspect. Ecol. Conserv.*, 15, 82-90. <https://doi.org/10.1016/j.pecon.2017.06.004>
- Arndal, M.F., Illeris, L., Michelsen, A., Albert, K., Tamstorf, M. and Hansen, B.U. (2009). Seasonal variation in gross ecosystem production, plant biomass, and carbon and nitrogen pools in five high arctic vegetation types. *Arctic, Arct. Antarct. Alp. Res.*, 41, 164-173. <https://doi.org/10.1657/1938-4246-41.2.164>
- Baldocchi, D.D., Black, T.A., Curtis, P.S., Falge, E., Fuentes, J.D., Granier, A., Gu, L., Knohl, A., Pilegaard, K., Schmid, H.P., Valentini, R., Wilson, K., Wofsy, S., Xu, L. and Yamamoto, S. (2005). Predicting the onset of net carbon uptake by deciduous forests with soil temperature and climate data: A synthesis of FLUXNET data. *Int. J. Biometeorol.*, 49, 377-387. <https://doi.org/10.1007/s00484-005-0256-4>
- Basler, D. and Körner, C. (2012). Photoperiod sensitivity of bud burst in 14 temperate forest tree species. *Agric. For. Meteorol.*, 165, 73-81. <https://doi.org/10.1016/j.agrformet.2012.06.001>
- Broich, M., Huete, A., Paget, M., Ma, X., Tulbure, M., Coupe, N.R., Evans, B., Beringer, J., Devadas, R., Davies, K. and Held, A. (2015). A spatially explicit land surface phenology data product for science, monitoring and natural resources management applications. *Environ. Model. Softw.*, 64, 191-204. <https://doi.org/10.1016/j.envsoft.2014.11.017>
- Browning, D.M., Karl, J.W., Morin, D., Richardson, A.D. and Tweedie, C.E. (2017). Phenocams bridge the gap between field and satellite observations in an arid grassland ecosystem. *Remote Sens.*, 9(10), 1071. <https://doi.org/10.3390/rs9101071>
- Churkina, G., Schimel, D., Braswell, B.H. and Xiao, X. (2005). Spatial analysis of growing season length control over net ecosystem exchange. *Glob. Change Biol.*, 11, 1777-1787. <https://doi.org/10.1111/j.1365-2486.2005.001012.x>
- Craine, J.M., Wolkovich, E.M., Towne, E.G. and Kembel S.W. (2012). Flowering phenology as a functional trait in a tallgrass prairie. *New Phytol.*, 193, 673-682. <https://doi.org/10.1111/j.1469-8137.2011.03953.x>
- Dai, J., Wang, H. and Ge, Q. (2014). The spatial pattern of leaf phenology and its response to climate change in China. *Int. J. Biometeorol.*, 58, 521-528. <https://doi.org/10.1007/s00484-013-0679-2>
- Do, F.C., Goudiaby, V.A., Gimenez, O., Diagne, A.L., Diouf, M., Rocheteau, A. and Akpo, L.E. (2005). Environmental influence on canopy phenology in the dry tropics. *For. Ecol. Manag.*, 215, 319-328. <https://doi.org/10.1016/j.foreco.2005.05.022>
- Dragoni, D., Schmid, H.P., Wayson, C.A., Potter, H., Grimmer, C.S.B. and Randolph, J.C. (2011). Evidence of increased net ecosystem productivity associated with a longer vegetated season in a deciduous forest in south-central Indiana, USA. *Glob. Change Biol.*, 17, 886-897. <https://doi.org/10.1111/j.1365-2486.2010.02281.x>
- Du, J., He, Z., Yang, J., Chen, L. and Zhu, X. (2014). Detecting the effects of climate change on canopy phenology in coniferous forests in semi-arid mountain regions of China. *Int. J. Remote Sens.*, 35, 6490-6507. <https://doi.org/10.1080/01431161.2014.955146>
- Fei, X., Jin, Y., Zhang, Y., Sha, L., Liu, Y., Song, Q., Zhou, W., Liang, N., Yu, G., Zhang, L., Zhou, R., Li, J., Zhang, S. and Li, P. (2017). Eddy covariance and biometric measurements show that a savanna ecosystem in Southwest China is a carbon sink. *Sci. Rep.*, 7, 41025. <https://doi.org/10.1038/srep41025>
- Fei, X., Song, Q., Zhang, Y., Liu, Y., Sha, L., Yu, G., Zhang, L., Duan, C., Deng, Y., Wu, C., Lu, Z., Luo, K., Chen, A., Xu, K., Liu, W., Huang, H., Jin, Y., Zhou, R., Li, J., Lin, Y., Zhou, L., Fu, Y., Bai, X., Tang, X., Gao, J., Zhou, W. and Grace, J. (2018). Carbon exchanges and their responses to temperature and precipitation in forest ecosystems in Yunnan, Southwest China. *Sci. Total Environ.*, 616-617, 824-840. <https://doi.org/10.1016/j.scitotenv.2017.10.239>
- Filippa, G., Cremonese, E., Migliavacca, M., Galvagno, M., Forkel, M., Wingate, L., Tomelleri, E., di Cella, U.M. and Richardson, A.D. (2016). Phenopix: A R package for image-based vegetation phenology. *Agric. For. Meteorol.*, 220, 141-150. <https://doi.org/10.1016/j.agrformet.2016.01.006>
- Fridley, J.D. (2012). Extended leaf phenology and the autumn niche in deciduous forest invasions. *Nature*, 485, 359-362. <https://doi.org/10.1038/nature11056>
- Gerst, K.L., Rossington, N.L. and Mazer, S.J. (2017). Phenological responsiveness to climate differs among four species of *Quercus* in North America. *J. Ecol.*, 105, 1610-1622. <https://doi.org/10.1111/1365-2745.12774>
- Gillespie, A.R., Kahle, A.B. and Walker, R.E. (1987). Color enhancement of highly correlated images. II. Channel ratio and 'chromaticity' transformation techniques. *Remote Sens. Environ.*, 22, 343-365. [https://doi.org/10.1016/0034-4257\(87\)90088-5](https://doi.org/10.1016/0034-4257(87)90088-5)
- Gilmanov, T.G., Soussana, J.F., Aires, L., Allard, V., Ammann, C., Balzarolo, M., Barcza, Z., Bernhofer, C., Campbell, C.L., Cernusca, A., Cescatti, A., Clifton-Brown, J., Dirks, B.O.M., Dore, S., Eugster, W., Fuhrer, J., Gimeno, C., Gruenwald, T., Haszpra, L., Hensen, A., Ibrom, A., Jacobs, A.F.G., Jones, M.B., Lanigan, G., Laurila, T., Lohila, A., Manca, G., Marcolla, B., Nagy, Z., Pilegaard, K., Pinter, K., Pio, C., Raschi, A., Rogiers, N., Sanz, M.J., Stefani, P., Sutton, M., Tuba, Z., Valentini, R., Williams, M.L. and Wohlfahrt, G. (2007). Partitioning European grassland net ecosystem CO<sub>2</sub> exchange into gross primary productivity and ecosystem respiration using light response function analysis. *Agric. Ecosyst. Environ.*, 121, 93-120. <https://doi.org/10.1016/j.agee.2006.12.008>
- Grace, J., José, J.S., Meir, P., Miranda, H.S. and Montes, R.A. (2006). Productivity and carbon fluxes of tropical savannas. *J. Biogeogr.*, 33, 387-400. <https://doi.org/10.1111/j.1365-2699.2005.01448.x>
- Güeswell, S., Furrer, R., Gehrig, R. and Pietragalla, B. (2017). Changes in temperature sensitivity of spring phenology with recent climate

- warming in Switzerland are related to shifts of the pre-season. *Glob. Change Biol.*, 23, 5189-5202. <https://doi.org/10.1111/gcb.13781>
- Hollinger, D.Y., Kelliher, F.M., Byers, J.N., Hunt, J.E., McSeveny, T. M. and Weir, P.L. (1994). Carbon dioxide exchange between an undisturbed old-growth temperate forest and the atmosphere. *Ecology*, 75(1), 134-150. <https://doi.org/10.2307/1939390>
- Ide, R., Nakaji, T., Motohka, T. and Oguma, H. (2011). Advantages of visible-band spectral remote sensing at both satellite and near-surface scales for monitoring the seasonal dynamics of GPP in a Japanese larch forest. *J. Agric. Meteorol.*, 67(2), 75-84. <https://doi.org/10.2480/agrmet.67.2.4>
- Ide, R. and Oguma, H. (2010). Use of digital cameras for phenological observations. *Ecol. Inform.*, 5, 339-347. <https://doi.org/10.1016/j.ecoinf.2010.07.002>
- Inoue, T., Nagai, S., Saitoh, T.M., Muraoka, H., Nasahara, K.N. and Koizumi, H. (2014). Detection of the different characteristics of year-to-year variation in foliage phenology among deciduous broad-leaved tree species by using daily continuous canopy surface images. *Ecol. Inform.*, 22, 58-68. <https://doi.org/10.1016/j.ecoinf.2014.05.009>
- Ito, A. (2010). Changing ecophysiological processes and carbon budget in East Asian ecosystems under near-future changes in climate: Implications for long-term monitoring from a process-based model. *J. Plant Res.*, 123, 577-588. <https://doi.org/10.1007/s10265-009-0305-x>
- Jin, C., Xiao, X., Merbold, L., Arneeth, A., Veenendaal, E. and Kutsch, W.L. (2013). Phenology and gross primary production of two dominant savanna woodland ecosystems in Southern Africa. *Remote Sens. Environ.*, 135, 189-201. <https://doi.org/10.1016/j.rse.2013.03.033>
- Joblove, G.H. and Greenberg, D. (1978). Color spaces for computer graphics. *Proceedings of the 5th Annual Conference on Computer Graphics and Interactive Techniques, SIGGRAPH 1978*, 20-25. <https://doi.org/10.1145/800248.807362>
- Julitta, T., Cremonese, E., Migliavacca, M., Colombo, R., Galvagno, M., Siniscalco, C., Rossini, M., Fava, F., Cogliati, S., di Cella, U.M. and Menzel, A. (2014). Using digital camera images to analyse snowmelt and phenology of a subalpine grassland. *Agric. For. Meteorol.*, 198-199, 116-125. <https://doi.org/10.1016/j.agrformet.2014.08.007>
- Kang, X., Hao, Y., Cui, X., Chen, H., Huang, S., Du, Y., Li, W., Kardol, P., Xiao, X. and Cui, L. (2016). Variability and changes in climate, phenology, and gross primary production of an alpine wetland ecosystem. *Remote Sens.*, 8(5), 391. <https://doi.org/10.3390/rs8050391>
- Keenan, T.F., Gray, J., Friedl, M.A., Toomey, M., Bohrer, G., Hollinger, D.Y., Munger, J.W., O'Keefe, J., Schmid, H.P., Wing, I.S., Yang, B. and Richardson, A.D. (2014). Net carbon uptake has increased through warming-induced changes in temperate forest phenology. *Nat. Clim. Change*, 4, 598-604. <https://doi.org/10.1038/nclimate2253>
- Kikuzawa, K. (1991). A cost-benefit analysis of leaf habit and leaf longevity of trees and their geographical pattern. *Am. Nat.*, 138, 1250-1263.
- Kim, Y., Kimball, J.S., Zhang, K. and McDonald, K.C. (2012). Satellite detection of increasing Northern Hemisphere non-frozen seasons from 1979 to 2008: Implications for regional vegetation growth. *Remote Sens. Environ.*, 121, 472-487. <https://doi.org/10.1016/j.rse.2012.02.014>
- Kramer, K., Leinonen, I. and Loustau, D. (2000). The importance of phenology for the evaluation of impact of climate change on growth of boreal, temperate and Mediterranean forests ecosystems: An overview. *Int. J. Biometeorol.*, 44, 67-75. <https://doi.org/10.1007/s004840000066>
- Lim, C.H., An, J.H., Jung, S.H., Nam, G.B., Cho, Y.C., Kim, N.S. and Lee, C.S. (2018). Ecological consideration for several methodologies to diagnose vegetation phenology. *Environ. Res.*, 33, 363-377. <https://doi.org/10.1007/s11284-017-1551-3>
- Luo, Y., El-madany, T.S., Filippa, G., Ma, X.L., Ahrens, B., Carrara, A., Gonzalez-Cascon, R., Cremonese, E., Galvagno, M., Hammer, T.W., Pacheco-Labrador, J., Martin, M.P., Moreno, G., Perez-Priego, O., Reichstein, M., Richardson, A.D., Romermann, C. and Migliavacca, M. (2018). Using near-infrared-enabled digital repeat photography to track structural and physiological phenology in Mediterranean tree-grass ecosystems. *Remote Sens.*, 10(8), 1293. <https://doi.org/10.3390/rs10081293>
- Ma, X., Huete, A., Yu, Q., Coupe, N.R., Davies, K., Broich, M., Ratana, P., Beringer, J., Hutley, L.B., Cleverly, J., Boulain, N. and Eamus, D. (2013). Spatial patterns and temporal dynamics in savanna vegetation phenology across the north Australian tropical transect. *Remote Sens. Environ.*, 139, 97-115. <https://doi.org/10.1016/j.rse.2013.07.030>
- Ma, X., Huete, A., Yu, Q., Restrepo-Coupe, N., Beringer, J., Hutley, L.B., Kanniah, K.D., Cleverly, J. and Eamus, D. (2014). Parameterization of an ecosystem light-use-efficiency model for predicting savanna GPP using MODIS EVI. *Remote Sens. Environ.*, 154, 253-271. <https://doi.org/10.1016/j.rse.2014.08.025>
- Migliavacca, M., Galvagno, M., Cremonese, E., Rossini, M., Meroni, M., Sonnentag, O., Cogliati, S., Manca, G., Diotri, F., Busetto, L., Cescatti, A., Colombo, R., Fava, F., di Cella, U.M., Pari, E., Siniscalco, C. and Richardson, A.D. (2011). Using digital repeat photography and eddy covariance data to model grassland phenology and photosynthetic CO<sub>2</sub> uptake. *Agric. For. Meteorol.*, 151, 1325-1337. <https://doi.org/10.1016/j.agrformet.2011.05.012>
- Mizunuma, T., Koyanagi, T., Mencuccini, M., Nasahara, K.N., Wingate, L. and Grace, J. (2011). The comparison of several colour indices for the photographic recording of canopy phenology of fagus crenata Blume in eastern Japan. *Plant Ecol. Divers.*, 4, 67-77. <https://doi.org/10.1080/17550874.2011.563759>
- Mizunuma, T., Mencuccini, M., Wingate, L., Ogée, J., Nichol, C. and Grace, J. (2014). Sensitivity of colour indices for discriminating leaf colours from digital photographs. *Methods Ecol. Evol.*, 5, 1078-1085. <https://doi.org/10.1111/2041-210X.12260>
- Mizunuma, T., Wilkinson, M., Eaton, E.L., Mencuccini, M., Morison J.I.L. and Grace, J. (2013). The relationship between carbon dioxide uptake and canopy colour from two camera systems in a deciduous forest in southern England. *Funct. Ecol.*, 27, 196-207. <https://doi.org/10.1111/1365-2435.12026>
- Moore, C.E., Beringer, J., Donohue, R.J., Evans, B., Exbrayat, J.F., Hutley, L.B. and Tapper, N.J. (2018). Seasonal, interannual and decadal drivers of tree and grass productivity in an Australian tropical savanna. *Glob. Change Biol.*, 24, 2530-2544. <https://doi.org/10.1111/gcb.14072>
- Muraoka, H., Saigusa, N., Nasahara, K.N., Noda, H., Yoshino, J., Saitoh, T.M., Nagai, S., Murayama, S. and Koizumi, H. (2010). Effects of seasonal and interannual variations in leaf photosynthesis and canopy leaf area index on gross primary production of a cool-temperate deciduous broadleaf forest in Takayama, Japan. *J. Plant Res.*, 123, 563-576. <https://doi.org/10.1007/s10265-009-0270-4>
- Nagai, S., Ichie, T., Yoneyama, A., Kobayashi, H., Inoue, T., Ishii, R., Suzuki, R. and Itioka, T. (2016). Usability of time-lapse digital camera images to detect characteristics of tree phenology in a tropical rainforest. *Ecol. Inform.*, 32, 91-106. <https://doi.org/10.1016/j.ecoinf.2016.01.006>
- Nagai, S., Saitoh, T.M., Kurumado, K., Tamagawa, I., Kobayashi, H., Inoue, T., Suzuki, R., Gamo, M., Muraoka, H. and Nasahara, K.N. (2013a). Detection of bio-meteorological year-to-year variation by using digital canopy surface images of a deciduous broad-leaved forest. *SOLA*, 9, 106-110. <https://doi.org/10.2151/sola.2013-024>
- Nagai, S., Saitoh, T.M., Noh, N.J., Yoon, T.K., Kobayashi, H., Suzuki, R., Nasahara, K.N., Son, Y. and Muraoka, H. (2013b). Utility of information in photographs taken upwards from the floor of closed-

- canopy deciduous broadleaved and closed-canopy evergreen coniferous forests for continuous observation of canopy phenology. *Ecol. Inform.*, 18, 10-19. <https://doi.org/10.1016/j.ecoinf.2013.05.005>
- Park, C.K., Ho, C.H., Jeong, S.J., Lee, E.J. and Kim, J. (2017). Spatial and temporal changes in leaf coloring date of *Acer palmatum* and *Ginkgo biloba* in response to temperature increases in South Korea. *PLoS ONE*, 12, 1-19. <https://doi.org/10.1371/journal.pone.0174390>
- Piao, S., Liu, Q., Chen, A., Janssens, I.A., Fu, Y., Dai, J., Liu, L., Lian, X., Shen, M. and Zhu, X. (2019). Plant phenology and global climate change: Current progresses and challenges. *Glob. Change Biol.*, 25, 1922-1940. <https://doi.org/10.1111/gcb.14619>
- Picard, G., Quegan, S., Delbart, N., Lomas, M.R., Le Toan, T. and Woodward, F.I. (2005). Bud-burst modelling in Siberia and its impact on quantifying the carbon budget. *Glob. Change Biol.*, 11, 2164-2176. <https://doi.org/10.1111/j.1365-2486.2005.01055.x>
- Polgar, C.A. and Primack, R.B. (2011). Leaf-out phenology of temperate woody plants: From trees to ecosystems. *New Phytol.*, 191, 926-941. <https://doi.org/10.1111/j.1469-8137.2011.03803.x>
- Reichstein, M., Jung, M., Carvalhais, N., Mahecha, M., Beer, C. and Tomelleri, E. (2010). FLUXNET-From point to globe. *Fluxletter*, 3, 4-8.
- Richardson, A.D., Black, T.A., Ciais, P., Delbart, N., Friedl, M.A., Gombon, N., Hollinger, D.Y., Kutsch, W.L., Longdoz, B., Luyssaert, S., Migliavacca, M., Montagnani, L., Munger, J.W., Moors, E., Piao, S., Rebmann, C., Reichstein, M., Saigusa, N., Tomelleri, E., Vargas, R. and Varlagin, A. (2010). Influence of spring and autumn phenological transitions on forest ecosystem productivity. *Philos. Trans. R. Soc. B: Biol. Sci.*, 365, 3227-3246. <https://doi.org/10.1098/rstb.2010.0102>
- Richardson, A.D., Bailey, A.S., Denny, E.G., Martin, C.W. and O'Keefe, J. (2006). Phenology of a northern hardwood forest canopy. *Glob. Change Biol.*, 12, 1174-1188. <https://doi.org/10.1111/j.1365-2486.2006.01164.x>
- Richardson, A.D., Braswell, B.H., Hollinger, D.Y., Jenkins, J.P. and Ollinger, S.V. (2009). Near-surface remote sensing of spatial and temporal variation in canopy phenology. *Ecol. Appl.*, 19, 1417-1428. <https://doi.org/10.1890/08-2022.1>
- Richardson, A.D., Jenkins, J.P., Braswell, B.H., Hollinger, D.Y., Ollinger, S.V. and Smith, M.L. (2007). Use of digital webcam images to track spring green-up in a deciduous broadleaf forest. *Oecologia*, 152, 323-334. <https://doi.org/10.1007/s00442-006-0657-z>
- Richardson, A.D., Keenan, T.F., Migliavacca, M., Ryu, Y., Sonnentag, O. and Toomey, M. (2013). Climate change, phenology, and phenological control of vegetation feedbacks to the climate system. *Agric. For. Meteorol.*, 169, 156-173. <https://doi.org/10.1016/j.agrformet.2012.09.012>
- Saitoh, T.M., Nagai, S., Saigusa, N., Kobayashi, H., Suzuki, R., Nasahara, K.N. and Muraoka, H. (2012). Assessing the use of camera-based indices for characterizing canopy phenology in relation to gross primary production in a deciduous broad-leaved and an evergreen coniferous forest in Japan. *Ecol. Inform.*, 11, 45-54. <https://doi.org/10.1016/j.ecoinf.2012.05.001>
- Saleska, S.R., Didan, K., Huete, A.R. and da Rocha, H.R. (2007). Amazon forests green-up during 2005 drought. *Science*, 318, 612. <https://doi.org/10.1126/science.1146663>
- Shen, M., Piao, S., Cong, N., Zhang, G. and Janssens, I.A. (2015). Precipitation impacts on vegetation spring phenology on the Tibetan Plateau. *Glob. Change Biol.*, 21, 3647-3656. <https://doi.org/10.1111/gcb.12961>
- Sims, D.A. and Gamon, J.A. (2002). Relationships between leaf pigment content and spectral reflectance across a wide range of species, leaf structures and developmental stages. *Remote Sens. Environ.*, 81, 337-354. [https://doi.org/10.1016/S0034-4257\(02\)00010-X](https://doi.org/10.1016/S0034-4257(02)00010-X)
- Snyder, K.A., Wehan, B.L., Filippa, G., Huntington, J.L., Stringham, T.K. and Snyder, D.K. (2016). Extracting plant phenology metrics in a great basin watershed: Methods and considerations for quantifying phenophases in a cold desert. *Sensors*, 16. <https://doi.org/10.3390/s16111948>
- Sonnentag, O., Detto, M., Vargas, R., Ryu, Y., Runkle, B.R.K., Kelly, M. and Baldocchi, D.D. (2011). Tracking the structural and functional development of a perennial pepperweed (*Lepidium latifolium* L.) infestation using a multi-year archive of webcam imagery and eddy covariance measurements. *Agric. For. Meteorol.*, 151, 916-926. <https://doi.org/10.1016/j.agrformet.2011.02.011>
- Sonnentag, O., Hufkens, K., Teshera-sterne, C., Young, A.M., Friedl, M., Braswell, B.H., Milliman, T., O'Keefe, J. and Richardson, A.D. (2012). Digital repeat photography for phenological research in forest ecosystems. *Agric. For. Meteorol.*, 152, 159-177. <https://doi.org/10.1016/j.agrformet.2011.09.009>
- Tang, J., Körner, C., Muraoka, H., Piao, S., Shen, M., Thackeray, S.J. and Yang, X. (2016). Emerging opportunities and challenges in phenology: a review. *Ecosphere*, 7, 1-17. <https://doi.org/10.1002/ecs2.1436>
- Toomey, M., Friedl, M.A., Frolking, S., Hufkens, K., Klosterman, S., Sonnentag, O., Baldocchi, D.D., Bernacchi, C.J., Biraud, S.C., Bohrer, G., Brzostek, E., Burns, S.P., Coursolle, C., Hollinger, D.Y., Margolis, H.A., Mccaughey, H., Monson, R.K., Munger, J.W., Pallardy, S., Phillips, R.P., Torn, M.S., Wharton, S., Zeri, M. and Richardson, A.D. (2015). Greenness indices from digital cameras predict the timing and seasonal dynamics of canopy-scale photosynthesis. *Ecol. Appl.*, 25, 99-115. <https://doi.org/10.1890/14-0005.1>
- Nagai, S., Yoshitake, S., Inoue, T., Suzuki, R., Muraoka, H., Nasahara, K.N. and Saitoh, T.M. (2014). Year-to-year blooming phenology observation using time-lapse digital camera images. *J. Agric. Meteorol.*, 70, 163-170. <https://doi.org/10.2480/agrmet.D-13-00021>
- Vitasse, Y., François, C., Delpierre, N., Dufrêne, E., Kremer, A., Chuine, I. and Delzon, S. (2011). Assessing the effects of climate change on the phenology of European temperate trees. *Agric. For. Meteorol.*, 151, 969-980. <https://doi.org/10.1016/j.agrformet.2011.03.003>
- Vitasse, Y., Porté, A.J., Kremer, A., Michalet, R. and Delzon, S. (2009). Responses of canopy duration to temperature changes in four temperate tree species: relative contributions of spring and autumn leaf phenology. *Oecologia*, 161, 187-198. <https://doi.org/10.1007/s00442-009-1363-4>
- Walther, G.R., Post, E., Convey, P., Menzel, A., Parmesan, C., Beebee, T.J.C., Fromentin, J.M., Hoegh-Guldberg, O. and Bairlein, F. (2002). Ecological responses to recent climate change. *Nature*, 416, 389-396. <https://doi.org/10.1038/416389a>
- Westergaard-Nielsen, A., Lund, M., Hansen, B.U., Tamstorf, M.P. (2013). Camera derived vegetation greenness index as proxy for gross primary production in a low Arctic wetland area. *ISPRS J. Photogramm. Remote Sens.*, 86, 89-99. <https://doi.org/10.1016/j.isprsjprs.2013.09.006>
- White, M.A. and Nemani, R.R. (2003). Canopy duration has little influence on annual carbon storage in the deciduous broad leaf forest. *Glob. Chang. Biol.*, 9, 967-972. <https://doi.org/10.1046/j.1365-2486.2003.00585.x>
- Wingate, L., Ogeé, J., Cremonese, E., Filippa, G., Mizunuma, T., Migliavacca, M., Moisy, C., Wilkinson, M., Moureaux, C., Wohlfahrt, G., Hammerle, A., Hörtnagl, L., Gimeno, C., Porcar-Castell, A., Galvagno, M., Nakaji, T., Morison, J., Kolle, O., Knohl, A., Kutsch, W., Kolari, P., Nikinmaa, E., Ibrom, A., Gielen, B., Eugster, W., Balzarolo, M., Papale, D., Klumpp, K., Köstner, B., Grünwald, T., Joffre, R., Ourcival, J.M., Hellstrom, M., Lindroth, A., George, C., Longdoz, B., Genty, B., Levala, J., Heinesch, B., Sprintsin, M., Yakir, D., Manise, T., Guyon, D., Ahrends, H., Plaza-Aguilar, A., Guan, J.H. and Grace, J. (2015). Interpreting canopy development and physiology using a European phenology camera network at flux sites. *Biogeosciences*, 12, 5995-6015. <https://doi.org/10.5194/bg-12-5995-2015>

- Woebbecke, D.M., Meyer, G.E., Von Bargaen, K. and Mortensen, D.A. (1995). Color indices for weed identification under various soil, residue, and lighting conditions. *Trans. ASAE*, 38, 259-269. <https://doi.org/10.13031/2013.27838>
- Zhang, X., Jayavelu, S., Liu, L., Friedl, M.A., Henebry, G.M., Liu, Y., Schaaf, C.B., Richardson, A.D. and Gray, J. (2018). Evaluation of land surface phenology from VIIRS data using time series of PhenoCam imagery. *Agric. For. Meteorol.*, 256-257, 137-149. <https://doi.org/10.1016/j.agrformet.2018.03.003>
- Zhao, J., Zhang, Y., Tan, Z., Song, Q., Liang, N., Yu, L. and Zhao, J. (2012). Using digital cameras for comparative phenological monitoring in an evergreen broad-leaved forest and a seasonal rain forest. *Ecol. Inform.*, 10, 65-72. <https://doi.org/10.1016/j.ecoinf.2012.03.001>
- Zhou, R., Zhang, Y., Song, Q., Lin, Y., Sha, L., Jin, Y., Liu, Y., Fei, X., Gao, J., He, Y., Li, T. and Wang, S. (2019). Relationship between gross primary production and canopy colour indices from digital camera images in a rubber (*Hevea brasiliensis*) plantation, Southwest China. *For. Ecol. Manag.*, 437, 222-231. <https://doi.org/10.1016/j.foreco.2019.01.019>